

Resonant enhancement of thermally-activated chemical reactions via vibrational polaritons

Jorge A. Campos Gonzalez Angulo, Raphael F. Ribeiro, and Joel Yuen-Zhou*

Department of Chemistry and Biochemistry. University of California San Diego. La Jolla, California 92093, USA

In the regime of ensemble vibrational strong coupling (VSC), a large number $N \gg 1$ of molecular transitions couple to each cavity mode, yielding two hybrid light-matter (polariton) modes, and a macroscopic reservoir of $N - 1$ dark states whose chemical dynamics are essentially those of the bare molecules. This fact is seemingly in opposition to the recently reported thermal activation of ground electronic state reactions under VSC. Here, we provide a VSC Marcus-Levich-Jortner electron transfer model that potentially addresses this paradox: while thermal equilibrium may entropically favor the population of dark-state channels, the chemical kinetics can be dictated by a few polaritonic channels with smaller activation energies. The effects of VSC reaction enhancement are maximal at light-matter resonance, in agreement with experimental observations.

When the excitations in a material medium interact strongly with a resonant confined electromagnetic mode, new states with light-matter hybrid character (polaritons) are formed[1, 2]. Recent studies of molecular polaritons have revealed new phenomena and features that make them promising for applications in chemistry and materials-science, opening doors to an emerging field of “polariton chemistry” [3–11]. Of particular interest to these studies are recent observations of chemoselective suppression and enhancement of reactive pathways for molecules whose high-frequency vibrational modes are strongly coupled to optical cavities [12–15]. These effects of vibrational strong coupling (VSC) are noteworthy in that they occur in the absence of external photon pumping, implying that they involve thermally-activated processes, and potentially opening doors to a radically new synthetic chemistry strategy that involves injecting microfluidic solutions in suitable optical cavities to induce desired transformations. It is important to highlight that the VSC in these samples is the consequence of an ensemble effect: each cavity mode couples to a large number of molecules, leading to two polaritonic modes and a macroscopic set of quasi-degenerate dark (subradiant) modes that, to a good approximation[16], should feature indistinguishable chemical dynamics compared to bare molecular modes[17]. At thermal equilibrium, a tiny fraction of vibrationally excited population would be allocated to polariton modes, with the overwhelming majority residing in the dark-state reservoir[18–20]. It is thus puzzling and remarkable that macroscopic differences in the chemical kinetics can be detected in systems under VSC. In this letter, we provide a possible rationale for these observations. By studying a VSC version of the well-established Marcus-Levich-Jortner (MLJ) thermally-activated electron transfer model [21–23], we find a parameter range where, even if the number of dark-state channels massively outweigh the few polaritonic ones, the latter dictate the kinetics of the reaction

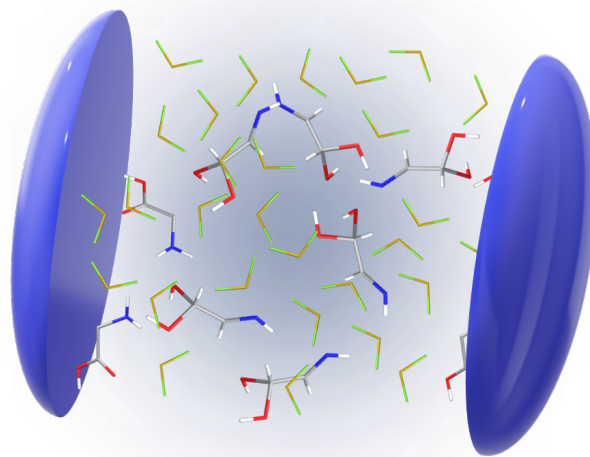


FIG. 1. Depiction of a microcavity encasing a large number of molecules that can undergo a chemical reaction (e.g. intramolecular electron transfer) and support a high frequency vibrational mode that can strongly couple to a confined optical mode; these molecules are in a solvated environment (green/yellow moieties). The reaction of concern is mediated by that intramolecular mode and a low frequency collective configuration of the solvation sphere.

given their smaller activation energies. Our model does not feature the complexity of the experimentally studied systems. However, it provides a minimalistic conceptual framework to develop qualitative insights on other thermally-activated VSC processes, for which we believe this polaritonic activation barrier reduction mechanism might be a widespread feature.

According to MLJ theory, the rate of charge-transfer between a donor (R) and an acceptor (P) is given by

* joelyuen@ucsd.edu

[21–23]

$$k_{R \rightarrow P} = \sqrt{\frac{\pi}{\lambda_S k_B T}} \frac{|J_{RP}|^2}{\hbar} e^{-S} \times \sum_{v=0}^{\infty} \frac{S^v}{v!} \exp\left(-\frac{(\Delta E + \lambda_S + v\hbar\omega_P)^2}{4\lambda_S k_B T}\right), \quad (1)$$

where J_{RP} is the electronic coupling between donor and acceptor, λ_S is the reorganization energy of a collective low-frequency (classical) mode related to the degrees of freedom of the solvent, ω_P is the frequency of a high-frequency intramolecular (quantum) mode whose quantum number is labeled by v , $S = \lambda_P/\hbar\omega_P$ is a Huang-Rhys parameter with λ_P the reorganization energy of the quantum mode, and ΔE is the energy gap between the zero-point energy levels of the donor and acceptor potential energy surfaces. The MLJ rate can be thought of as a generalization of the Marcus theory to include a sum of over channels with different quanta v in the high-frequency mode of the product.

To gauge the effects of VSC, we consider the interaction between a single microcavity mode and an ensemble of N acceptor-donor pairs that undergo electron transfer. For simplicity, we assume that VSC occurs via the high-frequency mode of P (if this coupling happens also through R , the conclusions do not qualitatively change). The Hamiltonian for such system is

$$\hat{H} = \hat{H}_{\text{ph}} + \sum_{i=1}^N \left[\hat{H}_R^{(i)} |R_i\rangle\langle R_i| + (\hat{H}_P^{(i)} + \hat{V}_{\text{int}}^{(i)}) |P_i\rangle\langle P_i| + J_{RP}(|R_i\rangle\langle P_i| + |P_i\rangle\langle R_i|) \right], \quad (2)$$

where $\hat{H}_{\text{ph}} = \hbar\omega_0 \left(\hat{a}_0^\dagger \hat{a}_0 + \frac{1}{2} \right)$ is the Hamiltonian of the electromagnetic mode with frequency ω_0 , $|R_i\rangle$ and $|P_i\rangle$ denote the electronic (donor/acceptor) states of the i -th molecule, $\hat{H}_R^{(i)} = \hbar\omega_R \hat{\mathcal{D}}_i^\dagger \hat{\mathcal{S}}_i^\dagger \left(\hat{a}_i^\dagger \hat{a}_i + \frac{1}{2} \right) \hat{\mathcal{S}}_i \hat{\mathcal{D}}_i + \hat{H}_S(\hat{q}_S^{(i)} + d_S)$ and $\hat{H}_P^{(i)} = \hbar\omega_P \left(\hat{a}_i^\dagger \hat{a}_i + \frac{1}{2} \right) + \hat{H}_S(\hat{q}_S^{(i)}) + \Delta E$ are the bare Hamiltonians of the i -th donor/acceptor with quantum mode frequency ω_R and ω_P , respectively. $\hat{V}_{\text{int}} = \hbar g \left(\hat{a}_i^\dagger \hat{a}_0 + \hat{a}_0^\dagger \hat{a}_i \right)$ is the light-matter interaction potential under the rotating wave approximation[24] with single-molecule coupling $g = -\mu\sqrt{\frac{\hbar\omega_0}{2V\varepsilon_0}}$, transition dipole moment μ , and cavity mode volume V , $\hat{H}_S(\hat{q}_S) = \frac{1}{2}\hbar\omega_S (\hat{p}_S^2 + \hat{q}_S^2)$ is the Hamiltonian of the classical mode with frequency ω_S , $\hat{a}_i^\dagger/\hat{a}_i$ are creation/annihilation operators acting on the quantum mode of the i -th molecule ($i = 0$ denotes the cavity mode), $\hat{\mathcal{S}}_i = \exp\left[\frac{1}{2}\ln\left(\sqrt{\frac{\omega_P}{\omega_R}}\right)(\hat{a}_i^{\dagger 2} - \hat{a}_i^2)\right]$ and $\hat{\mathcal{D}}_i = \exp\left[\frac{1}{\sqrt{2}}(\hat{a}_i^\dagger - \hat{a}_i)d_P\right]$ are squeezing and displacement operators[24], d_P and d_S are the rescaled distance between equilibrium configurations of the donor and acceptor along the quantum and classical mode coordinates,

respectively; and $\hat{p}_S^{(i)}$ and $\hat{q}_S^{(i)}$ are the rescaled momentum and position of the i -th classical mode. We shall point out that, since it only considers coupling to a single mode, the Hamiltonian in Eq. (2) entails coarse-graining; therefore, N is not the total number of molecules in the cavity volume, but the average of molecules coupled per cavity mode[18]. While polaritonic effects in electron transfer processes have been studied in the pioneering work of [25], we note that they were considered in the *electronic* strong coupling regime; as we shall see, the vibrational counterpart demands a different formalism and offers conceptually different phenomenology.

As a consequence of VSC, the system is best described in terms of collective normal modes defined by the operators[7, 25]

$$\begin{aligned} \hat{a}_{+(N)} &= \cos\theta_N \hat{a}_0 - \sin\theta_N \hat{a}_{B(N)}, \\ \hat{a}_{-(N)} &= \sin\theta_N \hat{a}_0 + \cos\theta_N \hat{a}_{B(N)}, \\ \hat{a}_{D(N)}^{(k)} &= \sum_{i=1}^N c_{ki} \hat{a}_i; \quad 1 \leq k \leq N-1 \end{aligned} \quad (3)$$

where the coefficients c_{ki} fulfill $\sum_{i=1}^N c_{ki} = 0$ and $\sum_{i=1}^N c_{k'i}^* c_{ki} = \delta_{k'k}$; these operators correspond to the upper and lower polaritons (UP , LP), and dark (D) modes, respectively. In Eq. (3), $\theta_N = \frac{1}{2} \arctan \frac{2g\sqrt{N}}{\Delta}$ is the mixing angle, where $\Delta = \omega_0 - \omega_P$ is the light-matter detuning, and $\hat{a}_{B(N)} = \frac{1}{\sqrt{N}} \sum_{i=1}^N \hat{a}_i$ corresponds to the so-called bright (superradiant) mode. These modes have associated frequencies

$$\begin{aligned} \omega_{\pm(N)} &= \frac{\omega_0 + \omega_P}{2} \pm \frac{\Omega_N}{2}, \\ \omega_D &= \omega_P, \end{aligned} \quad (4)$$

where $\Omega_N = \sqrt{4g^2 N + \Delta^2}$ is the effective Rabi splitting; equivalent definitions can be made for the creation operators. Note that there is no “free-lunch”: the super-radiantly enhanced VSC with the bright mode occurs at the expense of a macroscopic number of dark modes that do not mix with light.

Inside of the cavity, the reaction $R \rightarrow P$ becomes

$$\begin{aligned} R + UP_{N-1} + LP_{N-1} + \sum_{k=1}^{N-2} D_{N-1}^{(k)} \\ \rightarrow UP_N + LP_N + \sum_{k=1}^{N-1} D_N^{(k)}, \end{aligned} \quad (5)$$

where the subscripts indicate the number of molecules that participate in VSC. This reaction implies that each time a molecule transforms, it becomes part of the coupled ensemble.

The large degeneracy of dark modes hints that a judicious basis can be chosen to simplify calculations[26]. In particular, we shall consider the basis introduced in [27],

$$\hat{a}_D^{(k)} = \frac{1}{\sqrt{k(k+1)}} \left(\sum_{i=1}^k \hat{a}_i - k \hat{a}_{k+1} \right). \quad (6)$$

Notice that this mode is highly localized at \hat{a}_{k+1} but has a long tail for $\hat{a}_{1 \leq i \leq k}$ (for a visualization, see Fig. S1); furthermore, they are fully characterized by the index k , and thus independent of N . In terms of these dark modes, the reaction in Eq. (5) can be drastically simplified from an $N + 1$ to a three-body process,

$$R + UP_{N-1} + LP_{N-1} \longrightarrow UP_N + LP_N + D_{N-1}^{(N-1)}, \quad (7)$$

where, without loss of generality, we have implicitly considered that the N -th molecule is the one that undergoes the reaction. Furthermore, we can identify the normal modes of the photon (\hat{a}_0), the N -th molecule (\hat{a}_N), and

the bright state that excludes it ($\hat{a}_{B(N-1)}$) as natural degrees of freedom of the problem since the modes in reactants and products can be written in terms of these modes. Explicitly, for the reactants we have

$$\begin{pmatrix} \hat{a}_{+(N-1)} \\ \hat{a}_{-(N-1)} \end{pmatrix} = \begin{pmatrix} \cos \theta_{N-1} & -\sin \theta_{N-1} \\ \sin \theta_{N-1} & \cos \theta_{N-1} \end{pmatrix} \begin{pmatrix} \hat{a}_0 \\ \hat{a}_{B(N-1)} \end{pmatrix}, \quad (8)$$

$$\hat{a}'_N = \hat{D}_N^\dagger \hat{S}_N^\dagger \hat{a}_N \hat{S}_N \hat{D}_N, \quad (9)$$

where \hat{a}'_N acts on the vibrational degrees of freedom of the N -th reactant (see §S1 for a derivation); while for the products

$$\begin{pmatrix} \hat{a}_{+(N)} \\ \hat{a}_{-(N)} \\ \hat{a}_D^{(N-1)} \end{pmatrix} = \begin{pmatrix} \cos \theta_N & -\sin \theta_N & 0 \\ \sin \theta_N & \cos \theta_N & 0 \\ 0 & 0 & 1 \end{pmatrix} \begin{pmatrix} 1 & 0 & 0 \\ 0 & \sqrt{\frac{1}{N}} & \sqrt{\frac{N-1}{N}} \\ 0 & \sqrt{\frac{N-1}{N}} & -\sqrt{\frac{1}{N}} \end{pmatrix} \begin{pmatrix} \hat{a}_0 \\ \hat{a}_{B(N-1)} \\ \hat{a}_N \end{pmatrix}. \quad (10)$$

We note that the squeezing, displacement and rotation present in eqs. (8) to (10) can be regarded as either Duschinsky transformations in the position-momentum representation[28], or Doktorov operators in second quantization[29, 30].

With the above considerations, the VSC analogue of the MLJ rate in Eq. (1) is given by a sum over possible quanta $\{v_+, v_-, v_p\}$ in the product modes UP_N , LP_N and $D_{N-1}^{(N-1)}$, respectively,

$$k_{R \rightarrow P}^{VSC} = \sqrt{\frac{\pi}{\lambda_S k_B T}} \frac{|J_{RP}|^2}{\hbar} \sum_{v_+=0}^{\infty} \sum_{v_-=0}^{\infty} \sum_{v_D=0}^{\infty} W_{v_+, v_-, v_D}, \quad (11)$$

where $W_{v_+, v_-, v_D} = |F_{v_+, v_-, v_D}|^2 \exp\left(-\frac{E_{v_+, v_-, v_D}^\dagger}{k_B T}\right)$,

$$\begin{aligned} |F_{v_+, v_-, v_D}|^2 &= |\langle 0_{+(N-1)} 0_{-(N-1)} 0_R | v_+ v_- v_D \rangle|^2 \\ &= \left(\frac{\sin^2 \theta_N}{N}\right)^{v_+} \left(\frac{\cos^2 \theta_N}{N}\right)^{v_-} \left(\frac{N-1}{N}\right)^{v_D} \\ &\quad \times \left(\frac{v_+ + v_- + v_D}{v_+, v_-, v_D}\right) |\langle 0' | v_+ + v_- + v_D \rangle|^2 \end{aligned} \quad (12)$$

is a generic Franck-Condon factor between the global ground state in the reactants and the excited vibrational configuration in the product[27]. The calculation in Eq. (12) (see §S3 for a derivation) is reminiscent to the contemporary problem of boson sampling[31]. Using the notation from Eq. (1)

$$E_{v_+, v_-, v_D}^\dagger = \frac{(\Delta E_{v_+, v_-, v_D} + \lambda_S - \Delta E_R)^2}{4\lambda_S}, \quad (13)$$

is the activation energy of the channel, with $\Delta E_R = \frac{\hbar}{2} (\omega_{+(N-1)} + \omega_{-(N-1)} + \omega_R)$ and $\Delta E_{v_+, v_-, v_D} = \Delta E +$

$\hbar [\omega_{+(N)} (v_+ + \frac{1}{2}) + \omega_{-(N)} (v_- + \frac{1}{2}) + \omega_P (v_D + \frac{1}{2})]$. Eq. (12) affords a transparent physical interpretation: the state $|v_+ v_- v_D\rangle$ is accessed by creating $v_+ + v_- + v_D$ excitations in the oscillator of the N -th acceptor; there are $\binom{v_+ + v_- + v_D}{v_+, v_-, v_D}$ ways to do so; $\left(\frac{\sin^2 \theta_N}{N}\right)$, $\left(\frac{\cos^2 \theta_N}{N}\right)$, and $\left(\frac{N-1}{N}\right)$ are the projections of the product normal modes on the oscillator of the N -th acceptor.

Notably, when $\omega_R = \omega_P$ and $N \gg 1$, these quantities simplify to

$$|F_{v_+, v_-, v_D}|^2 = \frac{e^{-S}}{v_+! v_-! v_D!} \left(\frac{S \sin^2 \theta}{N}\right)^{v_+} \left(\frac{S \cos^2 \theta}{N}\right)^{v_-} S^{v_D}, \quad (14)$$

$$E_{v_+, v_-, v_D}^\dagger = \frac{[\Delta E + \lambda_S + \hbar(v_+ \omega_+ + v_- \omega_- + v_P \omega_P)]^2}{4\lambda_S}, \quad (15)$$

where we have dropped the dependence of angles and frequencies on N for brevity. For most of the experiments that achieve VSC[12, 17, 19, 32–35], the number of molecules that take part in the coupling per mode is between $N = 10^6$ to 10^{10} . For such orders of magnitude and, at first glance of Eq. (12) we would expect the contribution from the dark modes to dominate the rate, which according to Eq. (14) is the same as the bare case (Eq. (1)) for $v_+ = v_- = 0$, i.e., if the polaritons are not employed in the reaction. However, careful inspection of the expressions at hand hints to the existence of parameters ΔE and λ_S for which changes in the activation energy for the polariton channels dominate the rate. To achieve that, we need first that the contributions from the first transition outplay that between ground states,

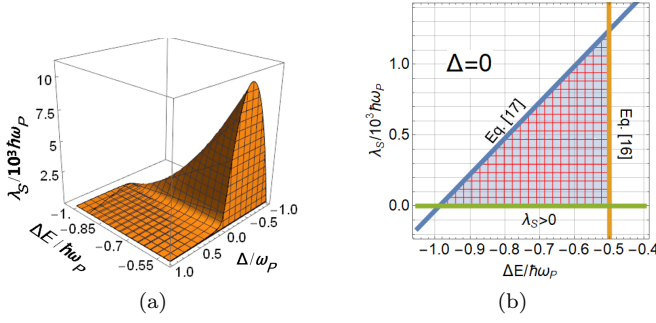


FIG. 2. Regions of parameters for which the lower polariton (LP) channel dominates the kinetics over the many dark (D) channels. ΔE is the energy difference between acceptor P and donor R and λ_S is the classical reorganization energy. For these calculations, the high frequency modes are equal $\omega_R = \omega_P$, $k_B T = 0.2\hbar\omega_P$ and the Rabi splitting is $\hbar\Omega = 5 \times 10^{-2}\hbar\omega_P$.

i.e., $W_{001} > W_{000}$, which implies

$$\frac{\lambda_P}{\hbar\omega_P} > \exp\left(\frac{\hbar\omega_P}{4\lambda_S k_B T} [2(\Delta E + \lambda_S) + \hbar\omega_P]\right). \quad (16)$$

Next, if the contribution from the channel to LP is to dominate, then $W_{010} > W_{001}$, which yields

$$\frac{N}{\cos^2 \theta} < \exp\left(\frac{\hbar(\Omega_N - \Delta)}{4\lambda_S k_B T} \times \left[\Delta E + \lambda_S + \hbar\omega_P + \frac{\hbar(\Delta - \Omega_N)}{4}\right]\right). \quad (17)$$

The region of parameters that satisfies these inequalities for room-temperature ($k_B T \approx 0.2\hbar\omega_P$) and typical experimental VSC Rabi-splittings $\hbar\Omega (\approx 0.1\hbar\omega_P)$ [12, 34] is illustrated in Fig. 2a. The order of magnitude of the plotted ΔE values is reasonably standard for this kind of processes [36, 37]; moreover, the requirement for very small λ_S is consistent with typical values of the classical frequency ω_S [23], which suggests the experimental feasibility of attaining these conditions.

The effect of the electromagnetic mode and the conditions for which the enhancement of the polaritonic coupling can be achieved is illustrated in Figure 3. We can understand it as follows; the reaction takes place as a multi-channel process where there is an electronic transition between the global ground state of the reactants and the states with vibrational excitations in the quantum mode of the product. As shown in Fig. S2, the channel between global ground states is in the Marcus inverted regime and, given the small value of the classical reorganization energy, the activation energy is fairly high. On the other hand, the channel to the first excited manifold is in the normal regime with a much lower activation energy, but the range of parameters implies that the decrease in activation energy for the channel leading to an excitation in the LP mode is enough to overcome the elevated multiplicity of the dark modes (Fig. S2). In

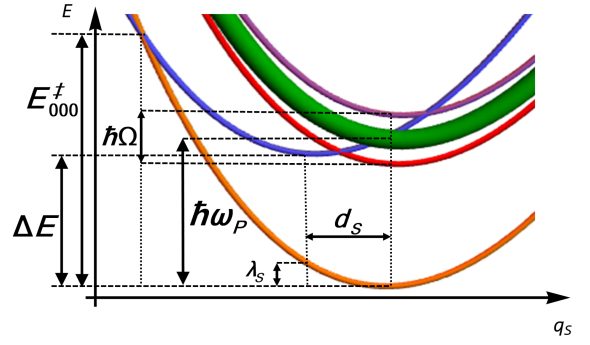


FIG. 3. Potential energy surfaces of the electronic states under VSC as a function of the slow coordinate q_S (not to scale). (a) With respect to the reactant (blue), the vibrational ground state of the product (orange) is in the Marcus inverted regime; the manifold of states with a vibrational excitation (green, red and purple) in the product is in the normal regime. While the dark states (green) outnumber the lower (red) and upper (purple) polaritons, the small activation energy associated to the lower polariton channel might make it the preferred pathway for reactivity.

terms of the expression of the rate constant, even though their dependence on N makes the pre-exponential factor of the D channel significantly larger than that of the LP channel, the converse is true –and has a more relevant effect– for the exponential factor.

In Fig. 2a we also show the change in the region of parameters as the detuning Δ varies. It can be noticed that the range of admissible values for the classical reorganization energy increases as the detuning becomes negative. This can be understood from the fact that, for negative detunings, the frequency of the photon is lower than that of the vibrational mode and, therefore, the activation energy to LP is lower than that corresponding to D , regardless of the intensity of the coupling (so long as it is finite), thus providing more flexibility for parameters to fulfill the inequalities in Eq. (17). The overall effect of the cavity in the charge transfer kinetics is displayed in Fig. 4 where we show the ratio of the rate constants, calculated inside ($k_{R \rightarrow P}$) and outside ($k_{R \rightarrow P}^{VSC}$) of the cavity as a function of the collective coupling, $g\sqrt{N}/\omega_P$, for several values of the detuning. The bell-shaped curves reflect the fact that, as the Rabi splitting increases, the activation energy of the LP decreases, thus making this channel the most prominent one. This trend goes on until $E_{010}^\ddagger = 0$, where this LP channel goes from the normal Marcus regime to the inverted one, and the activation energy starts to increase with the coupling until this pathway is rendered insignificant as compared to the transition to the D manifold, giving rise to kinetics indistinguishable from the bare molecules. The observation that larger detunings require stronger coupling to reach the maximum ratio of rate constants is consistent with the fact that $\hbar\Omega$ increases sublinearly with $\hbar g\sqrt{N}$; therefore, the larger the detuning, the slower the change. Additionally, the trend observed in the maxima, which

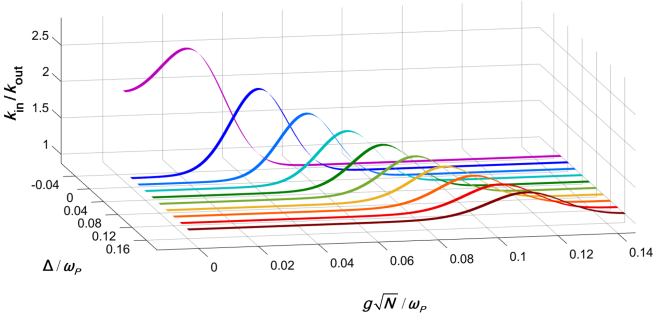


FIG. 4. Ratio between the rate constant inside the cavity, $k_{in} = k_{R \rightarrow P}^{VSC}$ with respect to the rate constant outside of the cavity $k_{out} = k_{R \rightarrow P}$ at several detunings Δ . For this calculations $\omega_R = \omega_P$, $k_B T = 0.2\hbar\omega_P$, $\hbar g = 1.6 \times 10^{-5}\hbar\omega_P$ and $E_{001}^\ddagger = 3.5\hbar\omega_P$. In agreement with Marcus theory, as the lower polariton channel lowers in energy (with increasing Rabi splitting), its corresponding activation energy falls and then rises, thus dominating the kinetics and becoming irrelevant, respectively.

decrease with the detuning, can be regarded as a consequence of both previous effects. The large couplings required to reach the zero-energy-barrier are due to a sizable number of molecules; therefore, the weight of D compared to that of LP becomes more relevant –as can be seen from the pre-exponential factors– and the effect is quenched. Finally, an outstanding result is the fact that the effect on the rate constant is more prominent in the few molecules regime for slightly negative detunings. This observation should not come as surprising since, as previously mentioned, under this condition the LP mode has a substantially decreased activation energy: therefore, for as small as it is, the coupling is enough to open a very favored channel that accelerates the reaction. Even though it might end washed out by dissipation processes, this observation perfectly illustrates why the abatement in activation energy has the potential to outmatch the high multiplicity of the dark mode manifold.

So far, we have shown that the rate constant depends on the number of molecules that take part in the VSC, which changes as the reaction progresses. To illustrate the overall effect on the kinetics, we numerically integrate the rate law

$$\frac{dN_R}{dt} = -k_{R \rightarrow P}^{VSC}(N_R)N_R \quad (18)$$

and show the behavior of $N_R(t) = N_R(t=0) - N(t)$ for several detunings in Fig. 5. In writing Eq. (18) we have assumed that every electron transfer event is accompanied by a much faster thermalization of the products (largely into the high-frequency mode ground state in the products side) that allows us to ignore back reactions. This assumption is well justified if we consider that, for systems with parameters close to our model molecule, the vibrational absorption linewidth is of the order of $0.05\hbar\omega_P$ [12, 34], which represents a timescale suitably shorter than the reaction times estimated so far. In Fig.

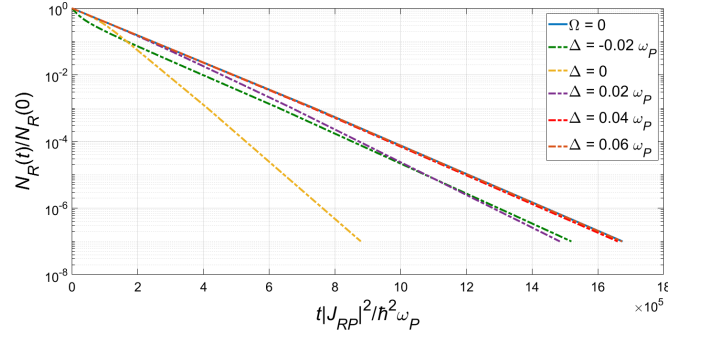


FIG. 5. Integrated rate law for the reaction outside and inside of the cavity at several detunings. For these calculations $\omega_R = \omega_P$, $k_B T = 0.2\hbar\omega_P$, and $E_{001}^\ddagger = 3.5\hbar\omega_P$. The departure of the VSC enhanced kinetics with respect to the bare case becomes more significant at resonance.

5 we can see that, for $\Delta \geq 0$, the reactions proceed in the same way as in the bare case, at early times. However, after some molecules have been gathered in the product, the coupling is strong enough for the LP channel to open and dominate over the D ones. This effect is cumulative, and the reaction endures a steady boost until the LP channel is closed (its activation energy becomes equal to that of D), thus restoring the bare behavior. In consistency with the experimental findings in [12–15], the maximum enhancement is observed for resonant conditions. On the other hand, with slightly negative detunings, the reaction is intensified in the early stages (as explained above) but is taken over by the dark states after a relatively short amount of time. In conclusion, even though some off-resonant effects might be present at the rate constant level, the condition of resonance is essential to observe a significant cumulative acceleration of the reaction (i.e., change in reactant lifetime) with respect to the bare case.

To summarize, we have shown that VSC can result in an acceleration in the kinetics of thermally-activated reactions. To assess this phenomenon, we have presented a generalized version of the MLJ model to study the enhancement of charge transfer processes under VSC (in passing, these results suggest a VSC alternative to enhance charge conduction processes that have so far been considered in the electronic strong coupling regime only [38–41]. In this model, there is a range of molecular features where the abatement of the activation energy in the lower polariton channel can outcompete the rate associated with the massive number of dark-state channels. We showed that these effects are most prominent under resonant conditions, consistently with recent experimental observations (we wish to mention a related theoretical study on off-resonant Casimir-Polder VSC effects on chemical reactivity[42]). While a thorough understanding of the reaction pathways involved in these observations is beyond the scope of this article, we believe that the tug-of-war between activation energy reduction from

few polariton channels against the domination of the kinetics by dark states could be a ubiquitous mechanism of thermally-activated polariton chemistry under VSC, independently of whether it occurs with reactants or products. While there might be other subtle physical mechanisms underlying VSC thermally-activated reactions, we conclude with three important observations regarding the presently proposed mechanism. First, it does not offer reduction of reaction rates; after all, if the polariton channels do not offer incentives for their utilization, the dark states will still be there, leading to virtually unaffected reaction rates as compared with the bare case. However, an experimental suppression of reactions by VSC under thermally-activated conditions (as in [12, 13]) could be, microscopically, a consequence of the polaritonic activation of a side reaction or process. Second, the conclusions associated to this mechanism do not strictly apply to photochemical processes where nonequilibrium initialization of polariton populations is allowed. Finally, it is important to emphasize that this VSC mechanism is not guaranteed to yield changes in thermally-activated reactivity given that particular geometric molecular conditions need to be fulfilled. Regardless, it is remarkable that thermally-activated reactions under VSC can be modified at all, given the entropic limitations imposed by the dark states. It is of much interest to the chemistry community to unravel the class of reactions and the VSC conditions for which this mechanism is operative; this will be part of our future work.

METHODS

To calculate the consumption of the reactant as the polaritonic ensemble grows, we performed a finite-difference numerical integration of Eq. (18), setting $dN_R \rightarrow \Delta N_R = -1$, and computing $\Delta t(N_R) = (k_{R \rightarrow P}^{VSC}(N_R)N_R)^{-1}$. The rate constant at each step is calculated from Eq. (11) truncating the sum up to $v_+ = v_- = v_D = 2$; terms beyond these excitations do not contribute appreciably given their huge activation energies resulting from the chosen parameters. The Franck-Condon and exponential factors are calculated, respectively, from Eqs. (12) and (13), setting $\omega_R = \omega_P$. Additionally, to enforce a weak coupling regime in the early stages, the frequencies of the cavity and acceptor modes are considered complex, with the imaginary part given by the corresponding linewidth ($\Gamma \approx 0.05\omega_P$) (ignoring this linewidth yields negligible differences in the cumulative kinetics, given that it only affects the early stages of the reaction).

Acknowledgements. The theoretical setup of the electron transfer reaction in terms of polariton and dark modes was carried out by J.A.C.G.A. with initial support of a UC-Mexus-CONACYT graduate scholarship. The calculations of Frank-Condon factors and development of the Marcus-Levich-Jortner model was carried out

by J.A.C.G.A. and R.F.R. under sponsorship of AFOSR award FA9550-18-1-0289. J.Y.Z. provided guidance on the interpretation of the results with support of NSF EAGER Award CHE 1836599. J.A.C.G.A thanks Matthew Du and Luis Martnez-Martnez for useful discussions.

-
- [1] J. J. Hopfield, PR **112**, 1555 (1958).
 - [2] V. M. Agranovich and A. G. Malshukov, Opt. Commun **11**, 169 (1974).
 - [3] T. W. Ebbesen, Acc. Chem. Res. **49**, 2403 (2016).
 - [4] K. Bennett, M. Kowalewski, and S. Mukamel, Faraday Discuss. **194**, 259 (2016).
 - [5] M. Sukharev and A. Nitzan, J. Phys. Condens. Matter **29**, 443003 (2017).
 - [6] D. G. Baranov, M. Wersll, J. Cuadra, T. J. Antosiewicz, and T. Shegai, ACS Photonics **5**, 24 (2018).
 - [7] R. F. Ribeiro, L. A. Martnez-Martnez, M. Du, J. Campos-Gonzalez-Angulo, and J. Yuen-Zhou, Chem. Sci. **9**, 6325 (2018).
 - [8] J. Flick, N. Rivera, and P. Narang, Nanophotonics **7**, 1479 (2018).
 - [9] K. Stranius, M. Hertzog, and K. Brjesson, Nat. Commun. **9**, 2273 (2018).
 - [10] M. Ruggenthaler, N. Tancogne-Dejean, J. Flick, H. Appel, and A. Rubio, Nat. Rev. Chem. **2**, 0118 (2018).
 - [11] J. Feist, J. Galego, and F. J. Garcia-Vidal, ACS Photonics **5**, 205 (2018).
 - [12] A. Thomas, J. George, A. Shalabney, M. Dryzhakov, S. J. Varma, J. Moran, T. Chervy, X. Zhong, E. Devaux, C. Genet, J. A. Hutchison, and T. W. Ebbesen, Angew. Chem. Int. Ed. **55**, 11462 (2016).
 - [13] A. Thomas, L. Lethuillier-Karl, K. Nagarajan, R. M. A. Vergauwe, J. George, T. Chervy, A. Shalabney, E. Devaux, C. Genet, J. Moran, and T. W. Ebbesen, Science **363**, 615 (2019).
 - [14] H. Hiura, A. Shalabney, and J. George, (2018), 10.26434/chemrxiv.7234721.v3.
 - [15] J. Lather, P. Bhatt, A. Thomas, T. W. Ebbesen, and J. George, ChemRxiv (2018).
 - [16] Ultrastrong coupling effects could potentially change this picture. However, these effects should not be significant for the modest Rabi splittings observed in the experiments [12–15] which concern us at present.
 - [17] A. D. Dunkelberger, R. B. Davidson, W. Ahn, B. S. Simpkins, and J. C. Owrutsky, J. Phys. Chem. A **122**, 965 (2018).
 - [18] J. del Pino, J. Feist, and F. J. Garcia-Vidal, New J. Phys. **17**, 053040 (2015).
 - [19] B. Xiang, R. F. Ribeiro, A. D. Dunkelberger, J. Wang, Y. Li, B. S. Simpkins, J. C. Owrutsky, J. Yuen-Zhou, and W. Xiong, Proc Natl Acad Sci USA **115**, 4845 (2018).
 - [20] J. Erwin, M. Smotzer, and J. V. Coe, J. Phys. Chem. B **123**, 1302 (2019).
 - [21] R. A. Marcus, Annu. Rev. Phys. Chem. **15**, 155 (1964).
 - [22] V. G. Levich, Adv. Electrochem. Eng. **4**, 249 (1966).
 - [23] J. Jortner, J. Chem. Phys. **64**, 4860 (1975).
 - [24] D. Walls and G. Milburn, *Quantum Optics* (Springer Berlin Heidelberg, 2008).
 - [25] F. Herrera and F. C. Spano, PRL **118**, 223601 (2017).
 - [26] E. J. Heller, *The Semiclassical Way to Dynamics and Spectroscopy* (Princeton University Press, 2018).

- [27] A. Strashko and J. Keeling, PRA **94**, 023843 (2016).
- [28] G. M. Sando, K. G. Spears, J. T. Hupp, and P. T. Ruhoff, J. Phys. Chem. A **105**, 5317 (2001).
- [29] E. V. Doktorov, I. A. Malkin, and V. I. Man'ko, J. Mol. Spectrosc. **77**, 178 (1979).
- [30] S. Banerjee and G. Gangopadhyay, J. Chem. Phys. **123**, 114304 (2005).
- [31] J. Huh, G. G. Guerreschi, B. Peropadre, J. R. McClean, and A. Aspuru-Guzik, Nat. Photonics **9**, 615 (2015).
- [32] J. P. Long and B. S. Simpkins, ACS Photonics **2**, 130 (2015).
- [33] A. Shalabney, J. George, J. Hutchison, G. Pupillo, C. Genet, and T. W. Ebbesen, Nat. Commun. **6**, 5981 (2015).
- [34] S. R. Casey and J. R. Sparks, J. Phys. Chem. C **120**, 28138 (2016).
- [35] R. M. A. Vergauwe, J. George, T. Chervy, J. A. Hutchison, A. Shalabney, V. Y. Torbeev, and T. W. Ebbesen, J. Phys. Chem. Lett. **7**, 4159 (2016).
- [36] S. Chaudhuri, S. Hedstrm, D. D. Mndez-Hernndez, H. P. Hendrickson, K. A. Jung, J. Ho, and V. S. Batista, J. Chem. Theory Comput. **13**, 6000 (2017).
- [37] F. Mirjani, N. Renaud, N. Gorczak, and F. C. Grozema, J. Phys. Chem. C **118**, 14192 (2014).
- [38] E. Orgiu, J. George, J. A. Hutchison, E. Devaux, J. F. Dayen, B. Doudin, F. Stellacci, C. Genet, J. Schachenmayer, C. Genes, G. Pupillo, P. Samor, and T. W. Ebbesen, Nat. Mater. **14**, 1123 (2015).
- [39] D. Hagenmiller, J. Schachenmayer, S. Schtz, C. Genes, and G. Pupillo, PRL **119**, 223601 (2017).
- [40] C.-Y. Cheng, R. Dhanker, C. L. Gray, S. Mukhopadhyay, E. R. Kennehan, J. B. Asbury, A. Sokolov, and N. C. Giebink, PRL **120**, 017402 (2018).
- [41] C. Mhl, A. Graf, F. J. Berger, J. Lttgens, Y. Zakharko, V. Lumsargis, M. C. Gather, and J. Zaumseil, ACS Photonics **5**, 2074 (2018).
- [42] J. Galego, C. Climent, F. J. Garcia-Vidal, and J. Feist, arXiv preprint arXiv:1807.10846 (2018).

Supplementary Material for “Resonant enhancement of chemical reactions via vibrational polaritons”

Jorge A. Campos Gonzalez Angulo, Raphael F. Ribeiro, and Joel Yuen-Zhou
Department of Chemistry and Biochemistry. University of California San Diego. La Jolla, California 92093, USA

S1 RELATION BETWEEN REACTANT AND PRODUCT HARMONIC OSCILLATOR OPERATORS

Let us consider the vibrational Hamiltonians for the single-molecule reactant and product electronic states (we omit label (i) for simplicity hereafter),

$$\hat{H}_R = \frac{\hat{p}^2}{2m} + \frac{m\omega_R^2 \hat{x}^2}{2} = \hbar\omega_R \left(\hat{a}_R^\dagger \hat{a}_R + \frac{1}{2} \right), \quad (\text{S1})$$

$$\hat{H}_P = \frac{\hat{p}^2}{2m} + \frac{m\omega_P^2 (\hat{x} - d_P)^2}{2} + \Delta E = \hbar\omega_P \left(\hat{a}_P^\dagger \hat{a}_P + \frac{1}{2} + \Delta E \right), \quad (\text{S2})$$

where m is the reduced mass of the mode, ω_A is the frequency of the mode in each electronic state ($A = R, P$), d_P is the difference between nuclear equilibrium configurations, ΔE is the energy difference between the electronic states, and \hat{p} and \hat{x} are the momentum and position operators for the described mode; therefore, the harmonic oscillator potential energy surface for P is a displaced-distorted version of that for R . The creation and annihilation operators are defined in terms of position and momentum ($d_R = 0$),

$$\begin{aligned} \hat{a}_A^\dagger &= \sqrt{\frac{\omega_A m}{2\hbar}} (\hat{x} - d_A) - \frac{i\hat{p}}{\sqrt{2\hbar\omega_A m}}, \\ \hat{a}_A &= \sqrt{\frac{\omega_A m}{2\hbar}} (\hat{x} - d_A) + \frac{i\hat{p}}{\sqrt{2\hbar\omega_A m}}; \end{aligned} \quad (\text{S3})$$

conversely, the position-momentum representation is written in terms of the creation and annihilation operators as

$$\begin{aligned} \hat{x} - d_A &= \sqrt{\frac{\hbar}{2\omega_A m}} (\hat{a}_A^\dagger + \hat{a}_A), \\ \hat{p} &= \sqrt{\frac{\hbar\omega_A m}{2}} i (\hat{a}_A^\dagger - \hat{a}_A). \end{aligned} \quad (\text{S4})$$

Eq. (S4) implies

$$\begin{aligned} \frac{\hat{a}_R^\dagger + \hat{a}_R}{\sqrt{\omega_R}} &= \frac{\hat{a}_P^\dagger + \hat{a}_P + \tilde{d}_P}{\sqrt{\omega_P}}, \\ \sqrt{\omega_R} (\hat{a}_R^\dagger - \hat{a}_R) &= \sqrt{\omega_P} (\hat{a}_P^\dagger - \hat{a}_P), \end{aligned} \quad (\text{S5})$$

where $\tilde{d}_P = \sqrt{2m/\hbar} d_P$; therefore, the reactant operators are written in terms of product ones as

$$\begin{aligned} \hat{a}_R^\dagger &= \frac{1}{2} \left(\sqrt{\frac{\omega_R}{\omega_P}} + \sqrt{\frac{\omega_P}{\omega_R}} \right) \hat{a}_P^\dagger + \frac{1}{2} \left(\sqrt{\frac{\omega_R}{\omega_P}} - \sqrt{\frac{\omega_P}{\omega_R}} \right) \hat{a}_P + \sqrt{\frac{\omega_R}{\omega_P}} \frac{\tilde{d}_P}{2}, \\ \hat{a}_R &= \frac{1}{2} \left(\sqrt{\frac{\omega_R}{\omega_P}} - \sqrt{\frac{\omega_P}{\omega_R}} \right) \hat{a}_P^\dagger + \frac{1}{2} \left(\sqrt{\frac{\omega_R}{\omega_P}} + \sqrt{\frac{\omega_P}{\omega_R}} \right) \hat{a}_P + \sqrt{\frac{\omega_R}{\omega_P}} \frac{\tilde{d}_P}{2}. \end{aligned} \quad (\text{S6})$$

These transformations can be written in terms of a squeezing and a displacement operator[1]:

$$\hat{S}_P(r) = \exp \left[\frac{r}{2} (\hat{a}_P^2 - \hat{a}_P^{\dagger 2}) \right], \quad (\text{S7})$$

$$\hat{D}_P(\alpha) = \exp \left[\alpha (\hat{a}_P^\dagger - \hat{a}_P) \right], \quad (\text{S8})$$

with actions given by

$$\hat{\mathcal{S}}_P^\dagger(r)\hat{a}_P^\dagger\hat{\mathcal{S}}_P(r) = \hat{a}_P^\dagger \cosh r - \hat{a}_P \sinh r, \quad (\text{S9})$$

$$\hat{\mathcal{D}}_P^\dagger(\alpha)\hat{a}_P\hat{\mathcal{D}}_P(\alpha) = \hat{a}_P + \alpha. \quad (\text{S10})$$

Therefore,

$$\begin{aligned} \hat{a}_R^\dagger &= \hat{\mathcal{D}}_P^\dagger(\alpha)\hat{\mathcal{S}}_P^\dagger(r)\hat{a}_P^\dagger\hat{\mathcal{S}}_P(r)\hat{\mathcal{D}}_P(\alpha) \\ \hat{a}_R &= \hat{\mathcal{D}}_P^\dagger(\alpha)\hat{\mathcal{S}}_P^\dagger(r)\hat{a}_P\hat{\mathcal{S}}_P(r)\hat{\mathcal{D}}_P(\alpha), \end{aligned} \quad (\text{S11})$$

for

$$r = \ln \sqrt{\frac{\omega_R}{\omega_P}}, \quad (\text{S12})$$

$$\alpha = \tilde{d}_P. \quad (\text{S13})$$

S2 VISUALIZATION OF QUASI-LOCALIZED BASIS OF DARK MODES

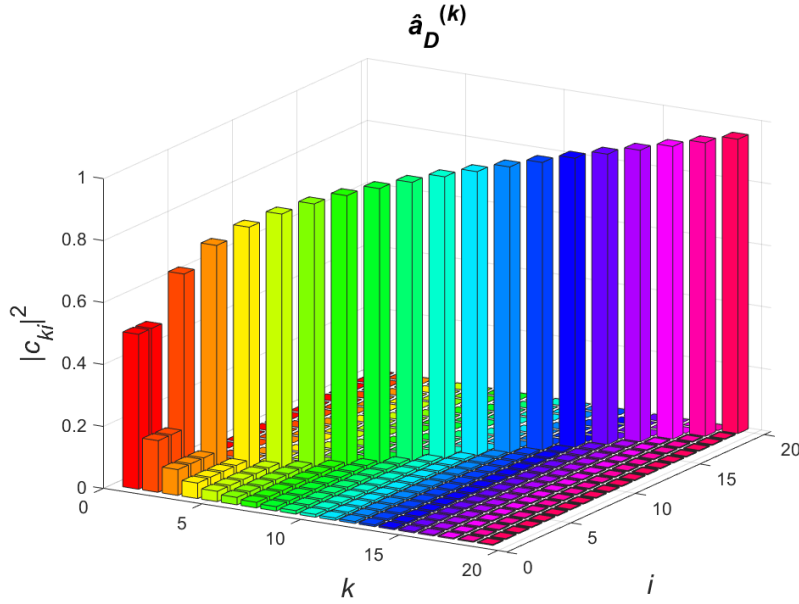


FIG. S1. Probability coefficients for each molecular mode in the quasi-localized basis of dark modes defined in Eq. 6. As the dark mode index, k , increases, it becomes more localized in the k -th molecule, leaving a long tail behind it.

S3 DERIVATION OF TRIDIMENSIONAL FRANCK-CONDON FACTOR IN EQ. (12)

The non-vanishing overlaps between the vibrational ground state of the reactants and an arbitrary vibrational excitation with quantum numbers $\{v_+, v_-, v_D\}$ on the products can be written in terms of creation operators as

$$\langle 0_0 0_{B/N} 0_R | v_+ v_- v_D \rangle = \langle 0_0 0_{B/N} 0_R | \frac{(\hat{a}_+^\dagger)^{v_+}}{\sqrt{v_+!}} \frac{(\hat{a}_-^\dagger)^{v_-}}{\sqrt{v_-!}} \frac{(\hat{a}_D^\dagger)^{v_D}}{\sqrt{v_D!}} | 0_+ 0_- 0_D \rangle. \quad (\text{S14})$$

These operators acting in the UP and LP can be written as linear combinations of the operators acting on the electromagnetic mode and the bright mode [Eq. 3], i.e.,

$$\langle 0_0 0_{B/N} 0_R | v_+ v_- v_D \rangle = \langle 0_0 0_{B/N} 0_R | \frac{(\hat{a}_0^\dagger \cos \theta - \hat{a}_B^\dagger \sin \theta)^{v_+} (\hat{a}_0^\dagger \sin \theta + \hat{a}_B^\dagger \cos \theta)^{v_-} (\hat{a}_D^\dagger)^{v_D}}{\sqrt{v_+! v_-! v_D!}} | 0_0 0_B 0_D \rangle \quad (\text{S15})$$

The binomial theorem yields

$$\begin{aligned} \langle 0_0 0_{B/N} 0_R | v_+ v_- v_D \rangle &= \frac{1}{\sqrt{v_+! v_-! v_D!}} \sum_{m=0}^{v_+} \sum_{n=0}^{v_-} \binom{v_+}{m} \binom{v_-}{n} \langle 0_0 0_{B/N} 0_R | \left(\hat{a}_0^\dagger \cos \theta \right)^m \left(-\hat{a}_B^\dagger \sin \theta \right)^{v_+ - m} \\ &\quad \times \left(\hat{a}_0^\dagger \sin \theta \right)^n \left(\hat{a}_B^\dagger \cos \theta \right)^{v_- - n} \left(\hat{a}_D^\dagger \right)^{v_D} | 0_0 0_{B/N} 0_D \rangle. \end{aligned} \quad (\text{S16})$$

Since $[\hat{a}_0, \hat{a}_B] = 0$, the only non-vanishing terms are those with $m = n = 0$, otherwise the overlap in the photonic mode would be between undisplaced states with different excitations, therefore

$$\langle 0_0 0_{B/N} 0_R | v_+ v_- v_D \rangle = \frac{1}{\sqrt{v_+! v_-! v_D!}} \langle 0_{B/N} 0_R | \left(-\hat{a}_B^\dagger \cos \theta \right)^{v_+} \left(\hat{a}_B^\dagger \sin \theta \right)^{v_-} \left(\hat{a}_D^\dagger \right)^{v_D} | 0_{B/N} 0_D \rangle. \quad (\text{S17})$$

Moreover, the creation operators acting on the bright and dark modes can be expressed as linear combinations of operators acting on the N -th molecule and the bright mode that excludes it [Eq. 6], i.e.,

$$\begin{aligned} \langle 0_0 0_{B/N} 0_R | v_+ v_- v_D \rangle &= \frac{(-\cos \theta)^{v_+} (\sin \theta)^{v_-}}{\sqrt{v_+! v_-! v_D!}} \langle 0_{B/N} 0_R | \left(\hat{a}_{B/N}^\dagger \sqrt{\frac{N-1}{N}} + \hat{a}_N^\dagger \sqrt{\frac{1}{N}} \right)^{v_+} \left(\hat{a}_{B/N}^\dagger \sqrt{\frac{N-1}{N}} + \hat{a}_N^\dagger \sqrt{\frac{1}{N}} \right)^{v_-} \\ &\quad \times \left(\hat{a}_{B/N}^\dagger \sqrt{\frac{1}{N}} - \hat{a}_N^\dagger \sqrt{\frac{N-1}{N}} \right)^{v_D} | 0_{B/N} 0_N \rangle. \end{aligned} \quad (\text{S18})$$

By expanding the binomials as before, and discarding the terms that excite the B/N mode, we arrive at to

$$\begin{aligned} \langle 0_0 0_{B/N} 0_R | v_+ v_- v_D \rangle &= \frac{(-\cos \theta)^{v_+} (\sin \theta)^{v_-}}{\sqrt{v_+! v_-! v_D!}} \langle 0_R | \left(-\hat{a}_N^\dagger \sqrt{\frac{1}{N}} \right)^{v_+} \left(\hat{a}_N^\dagger \sqrt{\frac{1}{N}} \right)^{v_-} \left(-\hat{a}_N^\dagger \sqrt{\frac{N-1}{N}} \right)^{v_D} | 0_N \rangle \\ &= \frac{1}{\sqrt{v_+! v_-! v_D!}} \left(-\frac{\cos \theta}{\sqrt{N}} \right)^{v_+} \left(\frac{\sin \theta}{\sqrt{N}} \right)^{v_-} \left(-\sqrt{\frac{N-1}{N}} \right)^{v_D} \langle 0_R | \left(\hat{a}_N^\dagger \right)^{v_+ + v_- + v_D} | 0_N \rangle. \end{aligned} \quad (\text{S19})$$

Acting the creation operator on the N -th mode allows us to write

$$\langle 0_0 0_{B/N} 0_R | v_+ v_- v_D \rangle = \sqrt{\frac{(v_+ + v_- + v_D)!}{v_+! v_-! v_D!}} \left(-\frac{\cos \theta}{\sqrt{N}} \right)^{v_+} \left(\frac{\sin \theta}{\sqrt{N}} \right)^{v_-} \left(-\sqrt{\frac{N-1}{N}} \right)^{v_D} \langle 0_R | (v_+ + v_- + v_D)_N \rangle. \quad (\text{S20})$$

Therefore, the square of the Franck-Condon factor in Eq. (S14) is

$$|\langle 0_0 0_{B/N} 0_R | v_+ v_- v_D \rangle|^2 = \binom{v_+ + v_- + v_D}{v_+, v_-, v_D} \left(\frac{\cos^2 \theta}{N} \right)^{v_+} \left(\frac{\sin^2 \theta}{N} \right)^{v_-} \left(\frac{N-1}{N} \right)^{v_D} |\langle 0_R | (v_+ + v_- + v_D)_N \rangle|^2. \quad (\text{S21})$$

S3 DIAGRAM OF ACTIVATION ENERGIES DUE TO VSC

[1] D. Walls and G. Milburn, *Quantum Optics* (Springer Berlin Heidelberg, 2008).

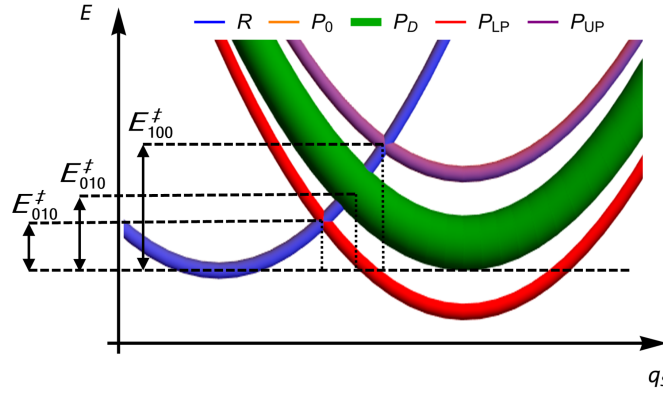


FIG. S2. Amplification of Fig. 3, showing a situation where a polariton channel dominates the kinetics of a reaction starting at reactant R . The channel involving a vibrational excitation in the lower polariton of the product (P_{LP}) features a small enough activation barrier E_{001}^\ddagger that it can efficiently compete against the many channels ending with a vibrational excitation in any of the dark modes, P_D , which feature corresponding activation energies E_{001}^\ddagger . These two activation energies are much smaller than E_{000}^\ddagger , the one associated to the channel leading to the global ground state of the products, P_0 .